Available online at www.sciencedirect.com
SCIENCE DIRECT®
Sensors and Actuators A 111 (2004) 260–266
SENSORS AND ACTUATORS A PHYSICAL
www.elsevier.com/locate/sna

Solid-phase conductive fuels for chemical microactuators

Heather H. DiBiaso, Brian A. English*, Mark G. Allen

Pettit Microelectronics Research Center, Georgia Institute of Technology, 791 Atlantic Drive, Atlanta, GA 30332, USA

Received 22 September 2003; received in revised form 27 October 2003; accepted 31 October 2003

Abstract

In this work, conductive, composite propellant-type, solid fuels are introduced and characterized for use in microactuators. Ignition was achieved with ammonium perchlorate-based fuels by passing electrical current through solid fuel compositions containing 20 vol.% graphite powder. Feasibility of this fuel is also demonstrated with the ignition of preliminary combustors. The fuels tested consist of ammonium nitrate, ammonium perchlorate, or sodium azide as the main fuel component, hydroxyl terminated polybutadiene or glycidyl azide polymer as the binder, various rate modifying additives including magnesium powder and submicron-sized aluminum powder, as well as graphite powder, which enables the fuel to become conductive. The resultant fuel mixture serves to simplify device fabrication by allowing ignition to occur by passing current directly through the fuel sample from two MEMS fabricated electrodes as opposed to relying on the transfer of heat from external or imbedded igniters. Results of burn time and conductivity testing indicate that the addition of approximately 20% graphite by volume enables conventional composite propellants to become conductive. Also, the addition of graphite roughly doubles the overall decomposition time in fuels containing hydroxyl terminated polybutadiene and only slightly increases overall decomposition time in fuels containing glycidyl azide polymer.

Keywords: Solid fuel; Conductive solid fuel; Gas-generating microactuator

1. Introduction

Historically, solid-phase composite propellants have been utilized as fuel for rocket boosters, as well as model rockets for hobbyists. In recent years, this type of fuel has been used in conjunction with IC and MEMS technologies to fabricate micron or millimeter-scale devices capable of producing tens of millinewtons of thrust [1–5]. These devices are often used for the attitude control of orbiting micro-spacecrafts. To produce such devices, the combustion chamber and igniter are fabricated separately. In general, the combustion chamber is bulk-etched from a silicon or ceramic substrate, while the igniter is formed by appropriately doping a polysilicon resistor. The two components are subsequently bonded together at the conclusion of the process. At this point, the solid fuel is packed into the microrocket device.

To ease the fabrication process of the actuator, MEMS fabrication techniques can be utilized to integrate the combustion chamber and the igniter. The work described in this paper explores solid-phase, conductive fuels that are ignited by passing current directly through the sample from two micromachined electrodes. In this case, the heat dissipated by the resistance of the fuel itself causes ignition.

This study modifies conventional composite propellants by adding an appropriate amount of graphite to the fuel mixture. Based on graphite loading of polyimide for micromachining applications [6], it was determined that the addition of approximately 20% powdered graphite by volume enabled conventional composite-type propellants to become conductive. The main fuel components that were studied include ammonium nitrate, ammonium perchlorate, and sodium azide. Several rate modifying components were also added to the mixtures to increase the reaction rate of the fuel. These components include magnesium, aluminum, potassium nitrate, and ammonium dichromate. Finally, hydroxyl terminated polybutadiene and glycidyl azide polymer were used as the binders.

2. Experimental procedures

2.1. Materials

Each of the chemicals utilized in this study was used as received unless otherwise noted. Ammonium nitrate prills were obtained from Fisher Scientific. These large prills were

* Corresponding author. Tel.: +1-770-2898272; fax: +1-404-8945028.
E-mail address: be25@prism.gatech.edu (B.A. English).

0924-4247/$ – see front matter © 2003 Elsevier B.V. All rights reserved.
doi:10.1016/j.sna.2003.10.062

later ground into smaller particles using a mortar and pestle. Phase-stabilized ammonium nitrate was obtained from CP Technologies in powder form. Ammonium perchlorate, in approximately 10 μm particle size and 90–180 μm particle size, was donated by the Aerospace Engineering department of Georgia Institute of Technology, and was ground using a mortar and pestle prior to use. Granular sodium azide was obtained from Alfa Aesar and also ground into finer particles with a mortar and pestle. Potassium nitrate, also in granular form, was obtained from Fisher Scientific. The magnesium powder came from Pyrotek and has a reported mesh size of 600–1000, and was used as received. Like the ammonium perchlorate, the aluminum powder was donated from Georgia Tech's Aerospace Engineering department and originated from Argonite. It is known as "Alex" and is a very fine, nano-particular powder with nominal particle size of 0.1 μm [7]. As with the magnesium powder, aluminum powder was also used as received. The powdered graphite that was used was obtained from Alfa Aesar and has a reported mesh size of −200. The polymeric binder, hydroxyl terminated polybutadiene, was obtained from CP Technologies while the energetic binder, glycidyl azide polymer, was acquired from Mach I Inc. The GAP was received as a mixture of 40% by volume polymer and 60% by volume ethyl acetate. For experimental use, the ethyl acetate was evaporated out of the solution. Ammonium dichromate catalyst, in crystalline form, was obtained from Fisher Scientific and was later ground into smaller particles using a mortar and pestle. Finally, the curing agent used, Mondur MR, came from CP Technologies. Mondur MR is a non-poisonous methyl diphenyl isocyanate curing agent. Throughout the remainder of this paper, the term "main fuel component" will be utilized to generally refer to ammonium nitrate, ammonium perchlorate, and/or sodium azide. All of the other components, except the binders, will be generally referred to as "rate modifying additives".

2.2. Sample preparation

Since this study was focused on fuel development, various experiments were performed to investigate the effect that the addition of graphite had on the overall burn time of composite propellant-type solid fuels. Propellant formulations of various compositions were prepared by hand in a 30 ml Pyrex beaker, and are listed in Table 1. For this experiment, each of the five representative formulations was packed by hand into the ceramic tile combustion chamber (6.8 mm × 6.8 mm × 0.5 mm) and topped with a 25 μm thick, IR-laser-machined, titanium igniter as illustrated in Fig. 1. After the igniter was pressed onto the surface of the unset fuel, it was allowed to cure at room temperature for 24 h. In this context, the term "unset" refers to a completely mixed fuel formulation that has not had sufficient time to cure. Upon curing, the fuel was tested for burn time using the following procedure.

Table 1
Composition of conductive fuels prepared and tested

Fuel component	wt.%	wt.%	wt.%	wt.%	wt.%
PSAN	37	0	0	0	0
AP	0	45	0	45	0
SA	0	0	45	0	50
HTPB	20	20	20	0	0
GAP	0	0	0	20	25
Mg	20	0	0	0	0
Alex	0	10	0	10	0
KNO_3	0	0	10	0	0
AD	3	0	0	0	0
Graphite	20	25	25	25	25
Total wt.%	100	100	100	100	100

2.3. Burn time testing procedure

First, a power supply was connected to the igniter using alligator clips. A DC power supply was used to supply the igniter with approximately 3.5 V. The voltage applied to the structure was determined from the maximum power that the igniter could dissipate without being destroyed. The next step was to place a Pyrex dish over the test structure to protect the microscope lens from any damage due to the combustion flame produced by the fuel. At this point, the test sample was prepared for video recording. The combustion

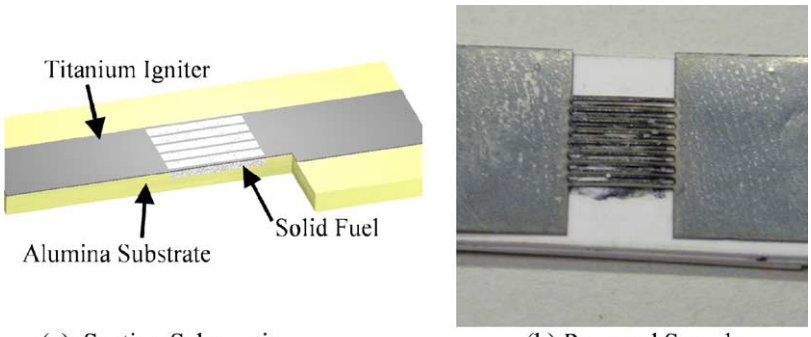

(a) Section Schematic (b) Prepared Sample

Fig. 1. Burn time test structure.

of each sample was recorded so that burn time could be ascertained at a later time. The test sample was then positioned under a low powered microscope equipped with a video camera. Next, the video capture system on the computer was initialized. To maximize the capture rate, the video was recorded using a 0.5 screen display (340 × 220 pixels), the capture rate was set to 30 frames per second, and the video was saved with no compression. Due to inadequacies of the capture system, however, a capture rate of 15 frames per second was actually observed. At this point, a stopwatch on the video feed was started and used to time the combustion. The video recording was started at the same time the power to the device was initiated. Upon the end of combustion, the video was saved and analyzed to determine burn time. Analysis of the burn time was done using Quicktime, Version Four. The combustion was viewed by advancing the video frame by frame, in 0.067 s increments. In this manner, the burn time was recorded. Burn time was defined as the time elapsed from the onset of the combustion flame to the end of combustion. To calculate burn rate, the actual sample thickness was divided by the burn time. For this calculation, the actual sample thickness was determined by dividing the sample mass by the product of the average density of the sample mass and the cross-sectional area of the chamber. Any excess fuel near the igniter should be sufficiently close to the igniter so as not to have a significant effect on the elapsed time that is recorded.

2.4. Conductivity testing procedure

The conductivity of each propellant formulation listed in Table 1 was also measured. For the conductivity tests, two separate combustion chambers were packed with fuel from the same mixture. These separate combustion chambers make-up trials one and two. The chambers used were identical to the chambers used to measure burn rate, however, metal electrodes were placed at either end of the combustion chamber, see Fig. 2. Conductivity testing was done by passing current through a piece of propellant of known dimensions (6.8 mm × 6.8 mm × 0.5 mm). Specifically, increasing voltage was applied to the propellant in small increments and the corresponding current was recorded. From these two values, the resistance of the fuel was calculated from Ohm's Law. This resistance was then converted to resistivity by Eq. (1):

$$R = \frac{\rho L}{A} \tag{1}$$

$$\sigma = \frac{1}{\rho} \tag{2}$$

The resistivity was then converted to conductivity by Eq. (2) and plotted as a function of applied volumetric power.

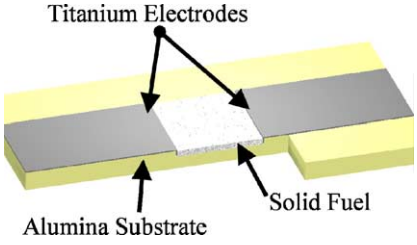

Fig. 2. Conductivity test sample schematic (section view).

3. Results and discussion

Each fuel listed in Table 1 was tested for conductivity and burn time as previously described. The burn time tests measure the effects of substituting graphite powder for oxidizer on the linear burn rate. The conductivity tests measured changes in resistance with respect to volumetric power input. During conductivity testing, an AP-based composition, 20% GAP, 10% Al, 25% graphite (20.07%, v/v), and 45% AP, ignited when 37 V was applied through the test sample. This same composition was later ignited using prototype combustors fabricated from Kapton and titanium.

3.1. Feasibility testing

The first fuel that was tested consisted of 25% GAP, 25% graphite, and 50% SA where all percentages are by weight. By volume, the formulation contained 19.34% graphite. Fig. 3 illustrates the measured conductivity as a function of applied volumetric power. To generate this figure, increasing voltage was applied to the fuel sample, and the corresponding current was recorded. Resistance was then calculated from Ohm's Law, and Eqs. (1) and (2) were subsequently used to calculate conductivity. Typically, resistance increases with increasing temperature when input power exceeded 25–50 W/cm^3. Therefore, the apparent decrease in conductivity with increasing voltage is most likely

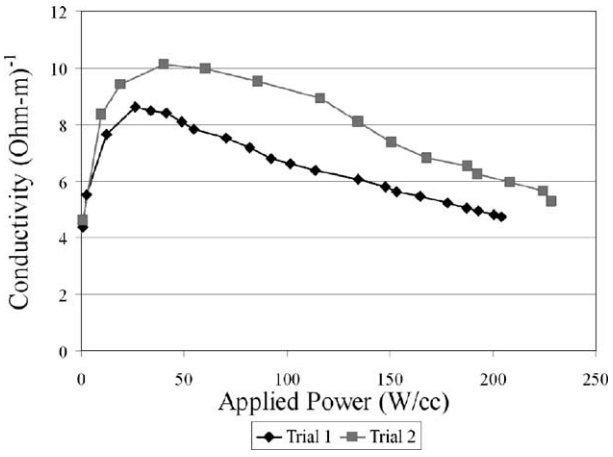

Fig. 3. Measured conductivity of 25 wt.% GAP, 25 wt.% graphite, and 50 wt.% SA.

Table 2
Burn time data for 25 wt.% GAP, 25 wt.% graphite, and 50 wt.% SA

Fuel formulation (wt.%)	Fuel weight (g)	Burn time (s)	Burn rate (mm/s)
25% GAP, 25% graphite, 50% SA	0.0456	0.46	1.09
25% GAP, 25% graphite, 50% SA	0.0442	0.47	1.06
25% GAP, 25% graphite, 50% SA	0.0435	0.34	1.47
25% GAP, 25% graphite, 50% SA	0.0434	0.47	1.06
Average	0.0442	0.44	1.17
Standard deviation	0.0010	0.06	0.17

a result of heat generated within the sample as the amount of current passed through it is increased.

The burn times were determined as described in the previous section and are summarized in Table 2. Since this initial formulation was mainly prepared to determine if conductivity was possible, a fuel containing the same components with the exception of graphite was not available to compare burn times to determine the effect of the graphite addition. It is, however, evident that the addition of 25 wt.% graphite did not prevent ignition.

3.2. Phase-stabilized ammonium nitrate

To effectively determine the impact of graphite on decomposition time, conventional fuel formulations were modified to include powdered graphite. These new formulations were also tested to determine their extent of conductivity. The first conductive fuel formulation that was prepared consisted of 20% HTPB, 20% Mg, 20% graphite (14.86%, v/v), 3% AD, and 37% PSAN. It should be noted that the fraction of oxidizer was reduced from its original 57% to compensate for the addition of graphite. Unfortunately, this fuel formulation was determined not to be conductive; no current was successfully passed through the sample. Furthermore, this particular fuel formulation did not ignite or achieve self-sustaining decomposition. Therefore, it was assumed that while increasing the fraction of graphite would have most likely mitigated the lack of conduction, further decreasing the oxidizer content would have been extremely detrimental to the fuel's ability to ignite. For this reason, it was decided that PSAN-based conductive fuels were unable to achieve both conductivity and adequate decomposition times.

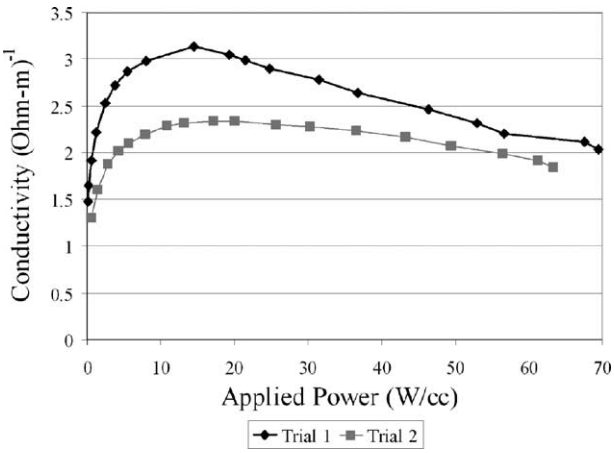

Fig. 4. Measured conductivity of 20 wt.% HTPB, 10 wt.% Al, 25 wt.% graphite, and 45 wt.%.

3.3. Ammonium perchlorate

The next fuel formulation that was tested consisted of 20% HTPB, 10% Al, 25% graphite (19.61%, v/v), and 45% AP. In this case, increasing the graphite content was possible because the oxidizer content was greater than in the PSAN-based fuel due to the necessity of fewer additives. Fig. 4 illustrates the results of this conductivity experiment. Like the conductivity results presented in Fig. 3, the conductivity of this fuel formulation also decreased when power input exceeded 20 W/cm^3. Again, this is most likely a result of increasing fuel temperature. Moreover, the burn time results of this fuel are presented in Table 3. As evident from this table, the addition of 25 wt.% graphite roughly doubled the observed decomposition time, i.e., halving the average linear burn rate. This phenomenon was most likely due to the

Table 3
Burn time comparison for an AP-based conductive fuel

Fuel Formulation (wt.%)	Fuel weight (g)	Burn time (s)	Burn rate (mm/s)
20% HTPB, 10% Al, 25% graphite, 45% AP	0.0464	0.47	1.06
20% HTPB, 10% Al, 25% graphite, 45% AP	0.0424	0.40	1.25
20% HTPB, 10% Al, 25% graphite, 45% AP	0.0450	0.47	1.06
20% HTPB, 10% Al, 25% graphite, 45% AP	0.0425	0.54	0.93
Average	0.0441	0.47	1.08
Standard deviation	0.0020	0.06	0.12
20% HTPB, 10% Al, 70% AP	0.0469	0.20	2.5
20% HTPB, 10% Al, 70% AP	0.0475	0.26	1.92
20% HTPB, 10% Al, 70% AP	0.0458	0.26	1.92
20% HTPB, 10% Al, 70% AP	0.0483	0.26	1.92
Average	0.0471	0.25	2.07
Standard deviation	0.0009	0.03	0.25

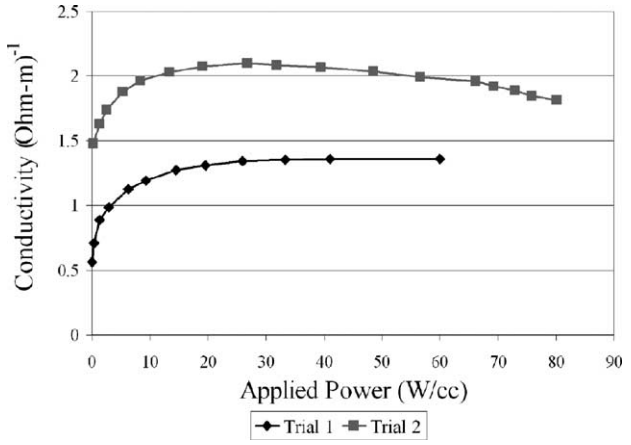

Fig. 5. Measured conductivity of 20 wt.% HTPB, 10 wt.% KNO_3, 25 wt.% graphite, and 45 wt.% SA.

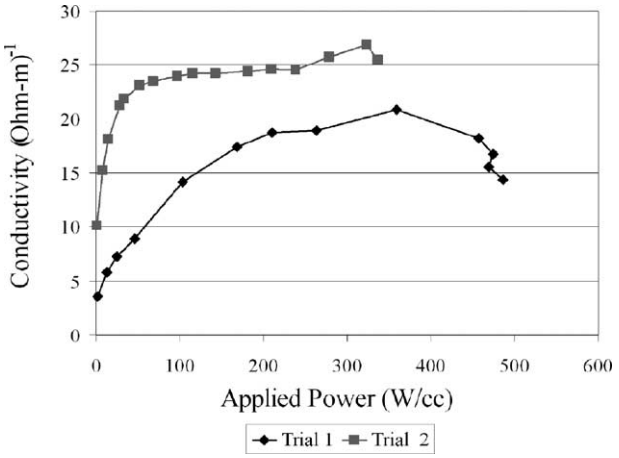

Fig. 6. Measured conductivity of 20 wt.% GAP, 10 wt.% Al, 25 wt.% graphite, and 45 wt.% AP.

decrease in mass fraction of the oxidizing agent as well as any heat-of-combustion energy lost to the post-combustion, sensible heating of graphite. However, despite the increase in burn time, the AP-based conductive fuel did ignite and achieved self-sustaining decomposition.

3.4. Sodium azide

Similar to the AP-based conductive fuel, an SA-based fuel was also made conductive by adding graphite. The data obtained for the fuel consisting of 20% HTPB, 10% KNO_3, 25% graphite (19.51%, v/v), and 45% SA is presented in Fig. 5. Yet again, the slight decrease in observed conductivity, when input power exceeded 20 W/cm^3, is, in all probability, due to the increasing temperature of the sample. The burn times associated with the SA-based conductive fuel are presented in Table 4 and are compared to their corresponding non-conductive SA-based fuel. Unfortunately, the SA-based conductive fuel was extremely difficult to ignite. Only one of the four samples that were attempted actually achieved self-sustaining combustion. Furthermore, the observed decomposition time was almost three times longer than its non-conductive counterpart, which is most likely due to the decrease in mass fraction of the main fuel component (NaN_3). The burn time of this fuel can also be compared to the burn time recorded for the first conductive fuel tested (25% GAP, 25% graphite, and 50% SA). In this case, the fuel containing 20% HTPB, 10% KNO_3, 25% graphite, and 45% SA burned five times slower. While the SA mass fraction was only 5% lower, the first conductive fuel contained the energetic binder, GAP. This additional energy source facilitates faster decomposition.

Table 4
Burn time comparison for an SA-based conductive fuel

Fuel formulation (wt.%)	Fuel weight (g)	Burn time (s)	Burn rate (mm/s)
20% HTPB, 10% KNO_3, 25% graphite, 45% SA	0.0403	2.2	0.23
Average	–	–	–
Standard deviation	–	–	–
20% HTPB, 10% KNO_3, 70% SA	0.0458	0.59	0.85
20% HTPB, 10% KNO_3, 70% SA	0.0464	0.67	0.75
20% HTPB, 10% KNO_3, 70% SA	0.0450	1.00	0.5
20% HTPB, 10% KNO_3, 70% SA	0.0458	0.87	0.57
20% HTPB, 10% KNO_3, 70% SA	0.0431	0.93	0.54
Average	0.0452	0.81	0.64
Standard deviation	0.0013	0.17	0.13

3.5. Energetic binder with ammonium perchlorate

With this in mind, another conductive fuel consisting of 20% GAP, 10% Al, 25% graphite (20.07%, v/v), and 45% AP was prepared and tested. The corresponding conductivity data is presented in Fig. 6. This formulation is almost eight times more conductive than its counterpart made with HTPB binder, which may be due to the different binders that were used. HTPB is classified as a non-conductive polymer; however, no such information was found regarding the electrical conductivity of GAP. Another important aspect to note is that the sample of AP-based conductive fuel containing GAP ignited when approximately 37 V was applied. No other conductive fuel achieved ignition during testing. A summary of the burn times measured for this conductive fuel is presented in Table 5. As opposed to the previous formulations, it can be seen that the addition of graphite only slightly increased the apparent burn time. Furthermore, of the five conductive fuel formulations prepared and tested, the fuel consisting of 20% GAP, 10% Al, 25% graphite, and 45% AP was found to be the most conductive and fastest burning.

3.6. Preliminary combustors

Preliminary devices have been tested using the following AP-based composition: 20% GAP, 10% Al, 25% graphite

Table 5
Burn time comparison for an AP-based conductive fuel containing GAP

Fuel Formulation (wt.%)	Fuel weight (g)	Burn time (s)	Burn rate (mm/s)
20% GAP, 10% Al, 25% graphite, 45% AP	0.0466	0.39	1.28
20% GAP, 10% Al, 25% graphite, 45% AP	0.0424	0.33	1.52
20% GAP, 10% Al, 25% graphite, 45% AP	0.0473	0.40	1.25
20% GAP, 10% Al, 25% graphite, 45% AP	0.0464	0.34	1.47
Average	0.0457	0.37	1.38
Standard deviation	0.0022	0.04	0.12
20% GAP, 10% Al, 70% AP	0.0417	0.40	1.25
20% GAP, 10% Al, 70% AP	0.0419	0.27	1.85
20% GAP, 10% Al, 70% AP	0.0438	0.27	1.85
20% GAP, 10% Al, 70% AP	0.0423	0.26	1.92
Average	0.0424	0.30	1.72
Standard deviation	0.0010	0.07	0.27

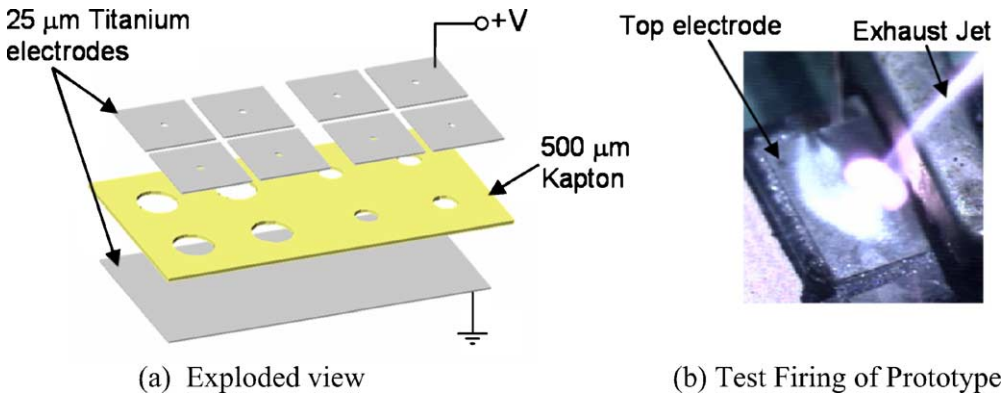

Fig. 7. Prototype combustor.

(20.07%, v/v), and 45% AP. Uncured solid fuel was packed into an intermediate layer of 500 μm thick Kapton, and then patterned titanium electrodes were attached via adhesive lamination. An exploded schematic may be seen in Fig. 7(a). The Kapton layer was patterned with four 5 mm diameter chambers and four 3 mm diameter chambers. The titanium nozzles were 0.5 mm in diameter and 25 μm thick. A 300 μF capacitor was charged to 130 V and then discharged into the combustion actuator. Fig. 7(b) shows the exhaust jet that resulted from this ignition.

4. Conclusions

From the data collected in this set of experiments, it was obvious that AP and SA-based fuels could successfully be made conductive by the addition of approximately 20% graphite by volume on an uncured basis. On the other hand, to achieve conductivity in PSAN-based fuels, it became necessary to decrease the oxidizer content to the point where the fuel lacked the ability to achieve satisfactory decomposition times. Moreover, the addition of graphite to conductive fuel formulations containing HTPB binder had a tendency to substantially increase the overall burn time, while conductive fuels containing GAP binder only slightly increased burn time. GAP-based conductive fuels also exhibited a higher degree of conductivity than HTPB-based conductive fuels. Finally, a sample of fuel consisting of 20% GAP, 25% graphite, 10% Al, and 45% AP was successfully ignited by passing current directly through the sample. Furthermore, the use of various conductive fuel formulations has been successfully demonstrated in preliminary MEMS combustors.

Acknowledgements

The authors would like to thank Defense Advanced Research Projects Agency (DARPA) for funding this research.

References

[1] C. Rossi, D. Esteve, C. Mingues, Pyrotechnic actuator: a new generation of Si integrated actuator, Sens. Actuators A: Phys. 74 (1999) 211–215.
[2] H. Helvajian (Ed.), Microengineering Aerospace Systems, The Aerospace Press, El Segundo, CA, 1999, pp. 637–696.

[3] D.H. Lewis Jr., S.W. Janson, R.B. Cohen, E.K. Antonsson, Digital MicroPropulsion, Sens. Actuators A: Phys. 80 (2000) 143–154.
[4] D. Teasdale, V. Milanovic, P. Chang, K.S.J. Pister, Microrockets for smart dust, Smart Mater. Struct. 10 (2001) 1145–1155.
[5] W. Lindsay, D. Teasdale, V. Milanovic, K. Pister, C. Fernandez-Pello, Thrust and Electrical Power from Solid Propellant Microrockets, in: Proceedings of the 14th IEEE International Conference on Micro Electro Mechanical Systems, Interlaken, Switzerland, 2001, pp. 606–610.
[6] A.B. Frazier, M.G. Allen, Piezoresistive graphite/polyimide thin films for micromachining applications, J. Appl. Phys. 73 (1993) 4428–4433.
[7] A. Dokhan, E.W. Price, R.K. Sigman, J.M. Seitzmann, The effect of Al particle size on the burning rate and residual oxide in aluminized propellants, Paper AIAA-2001-3581 at the 37th AIAA/ASME/SAE/ASEE Joint Propulsion Conference, Salt Lake City, UT, 8–11 July 2001.

Biographies

Heather H. DiBiaso received her BS in chemical engineering from the Pennsylvania State University in December of 2000 and her MS in chemical engineering from Georgia Institute of Technology in May 2003. Her graduate research focused on solid fuel development for gas-generating microactuators. She is currently employed at Delphi Delco Electronic Systems in Kokomo, Indiana working in a sensor development group.

Brian A. English received a bachelors of mechanical engineering (1997) and a masters of mechanical engineering (1999) from the Georgia Institute of Technology in Atlanta, Georgia. He is currently a PhD graduate student in the field of Microelectromechanical Systems, or MEMS. Current research interests may be summarized as lamination based fluid microactuators for use in aerodynamic boundary layer control. Brian is a student member of AIAA, ASME, and IEEE.

Mark G. Allen received the BA degree in chemistry, the BSE degree in chemical engineering and the BSE degree in E.E. from the University of Pennsylvania in 1984, and the SM degree and the PhD degree in microelectronic materials from Massachusetts Institute of Technology in 1986 and 1989, respectively. His research at Massachusetts Institute of Technology focused on micromachining techniques to create structures for the in situ measurement of mechanical properties and adhesion of thin films for use in microelectronic processing. He was also engaged in microsensors, microactuators, and in feedback-stabilized micromachined mirrors for laser applications. He joined the faculty of Georgia Institute of Technology after a postdoctoral appointment at Massachusetts Institute of Technology.